Proceedings of IMECE2008
2008 ASME International Mechanical Engineering Congress and Exposition
October 31-November 6, 2008, Boston, Massachusetts, USA

IMECE2008-68609

BUBBLE RISE AND DEPARTURE FROM A VISCOUS LIQUID FREE SURFACE

Mehran Mohammadi Farhangi
Graduate Student
Department of Mechanical Engineering,
Ferdowsi University of Mashhad, Iran
farhangi.mehran@gmail.com

Mohammad Passandideh-Fard
Assistant Professor
Department of Mechanical Engineering,
Ferdowsi University of Mashhad, Iran
mpfard@um.ac.ir

Behtash Bagherian
Graduate Student
Department of Mechanical Engineering,
Ferdowsi University of Mashhad, Iran
Behtash60@gmail.com

ABSTRACT

In this paper, the rising of a single bubble in a viscous liquid and its departure from the free-surface are simulated using a transient 2D/axisymmetric model. To predict the shape of the bubble deformation, the Navier-Stokes equations in addition to an advection equation for liquid volume fraction are solved. A modified Volume-of-Fluid (VOF) technique based on Youngs' algorithm is used to track the bubble deformation. To validate the model, the results of simulations for terminal rise velocity and bubble shape are compared with those of the experiments. Next, the effect of different parameters such as initial bubble radius, channel height, and liquid viscosity and surface tension on the shape and rise velocity of the bubble is investigated**.** Finally, the interaction of the bubble with the free surface during its departure from the liquid is simulated, and the results are compared qualitatively with experimental photographs.

INTRODUCTION

The dynamic behavior of two-phase flows is of great importance in various processes ranging from engineering applications to environmental phenomena. The presence of air bubbles in hydrodynamic systems often reveals many undesirable effects such as early erosion, loss of efficiency or flow irregularities.

Many industrial applications involve two-phase flows with or without mass (and/or heat) transfer. Examples in Chemical Engineering include bubble columns, loop reactors, agitated stirred reactors, flotation, or fermentation reactors. For the design of efficient two-phase reactors detailed knowledge of, say, Bubble sizes and shapes, slip velocities, internal circulation, Swarm behaviors are of fundamental importance. Numerical studies of two-phase flows are carried out to analyze the interface behavior of one air bubble moving or rising in a liquid. In the past decade a number of techniques, each with their own particular advantages and disadvantages, have been developed to simulate complex multi-fluid flow problems. Level set methods [1-5] are designed to minimize the numerical diffusion hampering shock-capturing methods and typically define the interface as the zero level set of a distance function from the interface. The advection of this distance function evolves with the local fluid velocity. Level set methods are conceptually simple and relatively easy to implement. When the interface is significantly deformed, level set methods suffer from loss of mass (volume) and hence loss of accuracy.

A well-known method for tracking the free surface of a liquid is Volume-of-Fluid (VOF) technique [6] where the computational domain is characterized by a scalar color function *f* whose value is one for a cell full of liquid and zero for an empty cell. A cell with a value between zero and one indicates a free-surface cell. In addition to the value of the color function the interface orientation needs to be determined, which follows from the gradient of the *f* function. Roughly two important classes of VOF methods can be distinguished with respect to the representation of the interface, namely simple line interface calculation (SLIC) and piecewise linear interface calculation (PLIC). Earlier works with VOF were generally based on the SLIC algorithm introduced by Noh and

Woodward [7] and the donor-acceptor algorithm published by Hirt and Nichols [8]. Modern VOF techniques include the PLIC method of Youngs [9]. The accuracy and capabilities of the older VOF algorithm such as the Hirt and Nicholas VOF method were studied by Rudman [10]. A drawback of these VOF methods for advecting gas bubbles is the so-called artificial (or numerical) coalescence of gas bubbles which occurs when their mutual distances is less than the size of the computational cell.

Front tracking methods [11-13] make use of markers (for instance triangles), connected to a set of points, to track the interface whereas a fixed or Eulerian grid is used to solve the Navier-stokes equations. This method is extremely accurate but also rather complex to implement due to the fact that dynamic re-meshing of the Lagrangian interface mesh is required and mapping of the Lagrangian data onto the Eulerian mesh has to be carried out. Difficulties arise when multiple interfaces interact where all require a proper sub-grid model. Contrary to most other methods, the automatic merging of interfaces does not occur in front tracking techniques due to the fact that a separate mesh is used to track the interface. This property is advantageous in case swarm effects in dispersed flows need to be studied. A 3D front tracking method was used by Van Sint Annaland et al. [14] to simulate a single bubble rising in water. The front tracking algorithm predicted reasonably well the rise velocity and aspect ratio of a single air bubble rising in water for diameters in the range of 1 mm to 7 mm.

Computational studies concerning the motion of a bubble near an infinite free surface are more abundant, though again not so plentiful as with the rigid boundary problem. Early studies in this area dating back to the Second World War are concerned with the motion of underwater explosion bubbles: for example, the work by Herring [15] and subsequent numerical study by Taylor [16]. These necessarily model the bubble as spherical and so the effects of buoyancy and nearby boundaries are to displace the bubble rather than deform its shape. One early consideration of the non-spherical motion of the bubble was performed by Lenoir [17], who employed a simple boundary integral technique to model the motion of the bubble. Blake and Gibson [18] employed an approximate integral equation technique to model the motion of the bubble and free surface. During expansion and early collapse, the calculated motion was shown to be in good agreement with experiments. However, upon formation of the liquid jet within the bubble, this model fails and calculations are ceased. Later work by Kucera and Blake [19] has shown such approximate methods to compare well with boundary integral studies for bubbles not too close to a boundary, with a reasonable agreement possible down to standoff distances of about two maximum bubble radii up until the time of jet formation. More recent calculations using these techniques may be found in Reference [20].

In this study, the interface of a bubble in a liquid during its rise and departure from the free-surface are simulated using a transient 2D/axisymmetric model. A modified Volume-of-Fluid (VOF) technique based on Youngs' algorithm is used to track the bubble deformation. To validate the model, numerical results are compared with those of the experiments for terminal rise velocity and bubble shape. The effect of different parameters such as initial bubble radius, channel height, and liquid viscosity and surface tension on the shape and rise velocity of the bubble is investigated**.**

NOMENCLATURE

de	equivalent bubble diameter
D	bubble diameter
f	fractional amount of liquid
g	gravitational acceleration
$\vec{V}$	Velocity
p	pressure
R	bubble radius
t	time
V_∞	terminal bubble rise velocity
$\Delta\rho$	density difference
Δp	pressure difference

Greek letters

μ	Viscosity
ρ	density
γ	surface tension
τ	viscous stress tensor

Dimensionless

M $(=\frac{\Delta\rho g \mu_l^4}{\rho_l^2 \gamma^3})$	Morton number
Eo $(=\frac{\Delta\rho g d_e^2}{\gamma})$	Eotvos number
Re $(=\frac{\rho_l U_t d_e}{\mu_l})$	Reynolds number
Ca $(=\frac{\mu\vec{V}}{\gamma})$	Capillary number
Bo $(=\frac{\Delta\rho g R_t^{\,2}}{\gamma})$	Bond number

Subscripts and superscripts

L	liquid phase
G	gas phase

NUMERICAL METHOD

The main issue regarding the developed model is the advection of the bubble interface using VOF method. In this section, we present a brief account of the numerical method. In modeling we can reasonably assume that the multi-fluid system studied in this paper is an isothermal system of two Newtonian,

incompressible and immiscible fluids. The flow governing equations are:

$$\vec{\nabla}\cdot\vec{V} = 0 \tag{1}$$

$$\frac{\partial\vec{V}}{\partial t} + \vec{\nabla}(\vec{V}\vec{V}) = -\frac{1}{\rho}\vec{\nabla}p + \frac{1}{\rho}\vec{\nabla}\cdot\vec{\tau} + \frac{1}{\rho}\vec{F}_b \tag{2}$$

where $\vec{V}$ is the velocity vector, p is the pressure, ρ is the density and $\overrightarrow{F_b}$ represents body forces acting on the fluid. The bubble interface is advected using VOF method by means of a scalar field f whose value is unity in the liquid phase and zero in the gas. When a cell is partially filled with liquid, f will have a value between zero and one.

$$f = \begin{cases} 1 & \text{in liquid} \\ > 0, < 1 & \text{at the liquid-gas interface} \\ 0 & \text{in gas} \end{cases} \tag{3}$$

The discontinuity in f is propagating through the computational domain according to:

$$\frac{df}{dt} = \frac{\partial f}{\partial t} + \vec{V}\cdot\vec{\nabla}f = 0 \quad \Rightarrow \quad (\frac{\partial f}{\partial t})_{exact} = -(\vec{V}.\vec{\nabla})f \tag{4}$$

Although the velocity field is divergence free, the term $(\vec{\nabla}\cdot\vec{V})$ has an order of $O(\varepsilon)$ in numerical solution. Therefore, in order to increase the accuracy of the numerical solution, Eq. 4 is used in the conservative form as

$$(\frac{\partial f}{\partial t})_{numerical} = -(\vec{V}.\vec{\nabla})f - (\vec{\nabla}\cdot\vec{V})f = -\vec{\nabla}\cdot(\vec{V}f) \tag{5}$$

where

$$(\frac{\partial f}{\partial t})_{exact} = (\frac{\partial f}{\partial t})_{numerical} + (\vec{\nabla}\cdot\vec{V})f \tag{6}$$

For the advection of volume fraction f based on Eq. 4, different methods have been developed such as SLIC, Hirt-Nichols and Youngs' PLIC [8]. The reported literature on the simulation of free-surface flows reveals that Hirt-Nichols method has been used by many researchers. In this study, however, we used Youngs' method [6, 8, 9], which is a more accurate technique. Assuming the initial distribution of f to be given, velocity and pressure are calculated in each time step by the following procedure.

The f advection begins by defining an intermediate value of f,

$$\tilde{f} = f^n - \delta t\vec{\nabla}\cdot(\vec{V}f^n) \tag{7}$$

Then it is completed with a "divergence correction"

$$f^{n+1} = \tilde{f} + \delta t(\vec{\nabla}\cdot\vec{V})f^n \tag{8}$$

A single set of equations is solved for both phases, therefore, density and viscosity of the mixture are calculated according to:

$$\begin{aligned} \rho &= f\rho_L + (1-f)\rho_G \\ \mu &= f\mu_L + (1-f)\mu_G \end{aligned}, \tag{9}$$

where subscripts L and G denote the liquid and gas, respectively, μ is the viscosity. New velocity field is calculated according to the two-step time projection method as follows. First, an intermediate velocity is obtained,

$$\frac{\tilde{\vec{V}} - \vec{V}^n}{\delta t} = -\vec{\nabla}\cdot(\vec{V}\vec{V})^n + \frac{1}{\rho^n}\vec{\nabla}\cdot\vec{\tau}^n + \vec{g}^n + \frac{1}{\rho^n}\vec{F}_b{}^n \tag{10}$$

The continuum surface force (CSF) method [6, 21] is used to model surface tension as a body force ($\overrightarrow{F_b}$) that acts only on interfacial cells. Pressure Poisson equation is then solved to obtain the pressure field,

$$\vec{\nabla}\cdot[\frac{1}{\rho^n}\vec{\nabla}p^{n+1}] = \frac{\vec{\nabla}\cdot\tilde{\vec{V}}}{\delta t} \tag{11}$$

Next, new time velocities are calculated by considering the pressure field implicitly,

$$\frac{\vec{V}^{n+1} - \tilde{\vec{V}}}{\delta t} = -\frac{1}{\rho^n}\vec{\nabla}p^{n+1} \tag{12}$$

RESULTS

As a first step, the model was subjected to several tests in order to validate its results. The first case considered was that of a single bubble during its rise in a liquid; a case for which experimental results are available in terms of terminal bubble rise velocity against its diameter. The measured data performed by Grace [22] for air bubbles in water is given as a diagram shown in Fig. 1. The default material properties used in the simulations are given in Table 1.

properties	water	air
density	ρ_l=998.2 kg/m^3	ρ_a=1.1222 kg/m^3
viscosity	μ_l=1002×10^{-6} kg/(m.s)	μ_a=18.24×10^{-6} kg/(m.s)
surface tension	γ =0.073 N/m	

Tab. 1: Material properties

An axisymmetric coordinate system was used in the model to simulate the deformation of the bubbles rising in a vertical tube. The tube diameter was assumed to be around four times as that of the bubble diameter in order to reduce the wall influence on bubble movement. Bubbles with diameter ranged from 0.8 mm to 10 mm were simulated; larger ones tend to break up before they reach their terminal velocity.

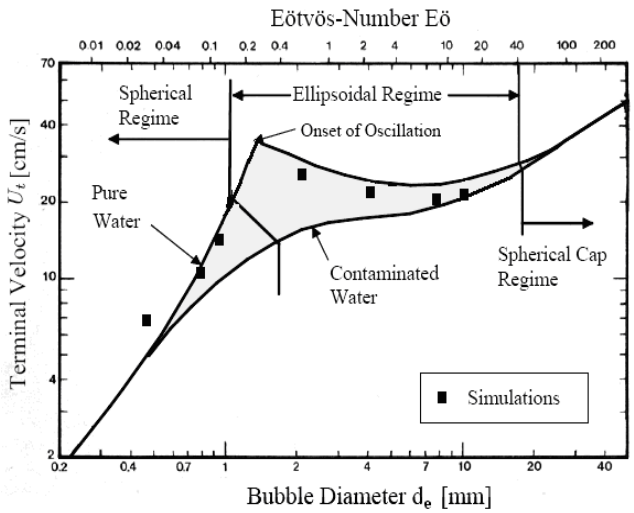

Fig. 1: A comparison between the results of simulations with those of the experiments [22] for terminal rise velocity against initial bubble diameter. Based on the experiments, the rise velocity should be located in the region surrounded by the solid lines.

The results of the model, presented in Fig. 1, are located in the same region where observed by experiments. The upper boundary of this region corresponds to pure systems, while the lower curve belongs to contaminated systems. As seen from the figure, increasing the bubble diameter increases the rise velocity up to a certain limit after which the bubble starts to oscillate. In this regime, the rise velocity remains nearly constant. Adding further to the bubble diameter changes the deformation behavior to the spherical cap regime where the rise velocity again increases with diameter.

For the bubbles smaller than the 0.5 mm there is an increasing deviation of simulated to measured velocities, which occurs mainly because of the so-called parasitic currents. These currents are due to inaccuracies in the calculation of surface tension forces, in particular because of errors in the interfacial normal and curvature.

MODEL VALIDATION

Grace [23] has analyzed a large body of experimental data on shapes and rise velocities of bubbles in quiescent viscous liquids and has shown that this data can be condensed into one diagram, provided that an appropriate set of dimensionless numbers is used. A representation of the Grace diagram [23] is shown in Fig. 2 where dimensionless numbers Morton (M), Eötvös (Eo), and Reynolds (Re) are given by

$$\mathrm{M}=\frac{\Delta\rho g\mu_l^4}{\rho_l^2\gamma^3}, \qquad \mathrm{Eo}=\frac{\Delta\rho g d_e^2}{\gamma}, \qquad \mathrm{Re}=\frac{\rho_l U_t d_e}{\mu_l} \quad (13)$$

where the equivalent diameter d_e is defined as the diameter of a spherical bubble with the same volume as that of the bubble under consideration. U_t represents the terminal rise velocity of the bubble.

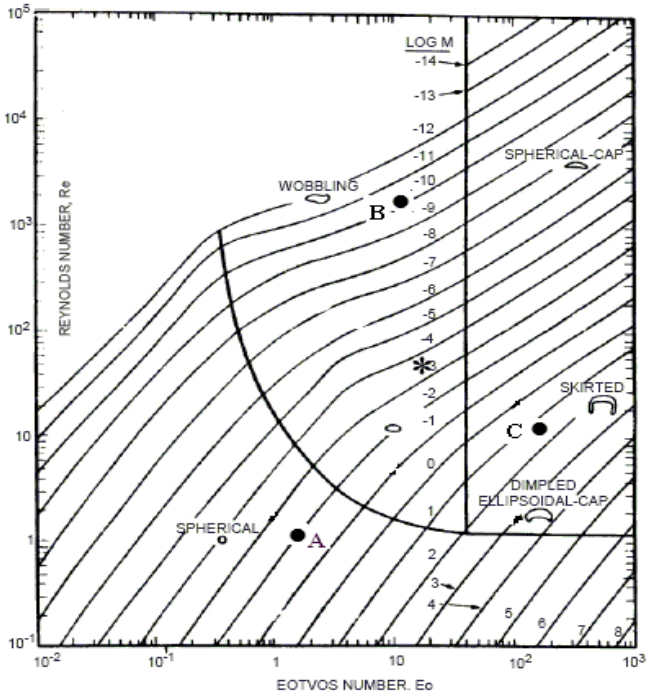

Fig. 2: Grace bubble diagram [23] for the shape and terminal rise velocity of gas bubbles in quiescent viscous liquids. Points A, B, and C show the cases for which the simulation results were compared with measurements as given in Table 2.

In Table 2, the values of the selected Morton and Eötvös numbers are given for simulations of bubbles in different regimes of bubble deformation. In this table, Re_{exp} and Re_{model} represent the bubble Reynolds numbers obtained from the Grace diagram and calculated from the model, respectively.

Bubble regime	**M**	**Eo**	**$\mathrm{Re}_{Exp.}$**	**Re_{Model}**	**Point (Fig. 2)**
spherical	1.42	0.01	1	1.2	A
wobbling	14.52	1×10^{-9}	2100	2200	B
skirted	142.56	1	15	18	C

Tab. 2: Morton (M) and Eötvös (Eo) numbers for simulations of bubbles in different regimes according to Grace bubble diagram [23].

Effect of Important Parameters

In this section, the effect of different parameters such as tube size, surface tension and viscosity on the shape and rise velocity of the bubble is investigated. In Fig. 3, the effect of tube diameter on the bubble shape and terminal rise velocity is shown. Velocity distributions along with flow streamlines at a time instant are also displayed in the figure. Free-slip boundary conditions were applied at all confining walls. As seen from the figure, increasing the tube diameter increases the rise velocity

characterized by Reynolds number. The data used for this simulation is given in Table 3. The density and viscosity ratio in this simulation is believed to be sufficiently high to mimic gas–liquid systems with sufficient accuracy and much higher than the ratio used by Sabisch et al. [24].

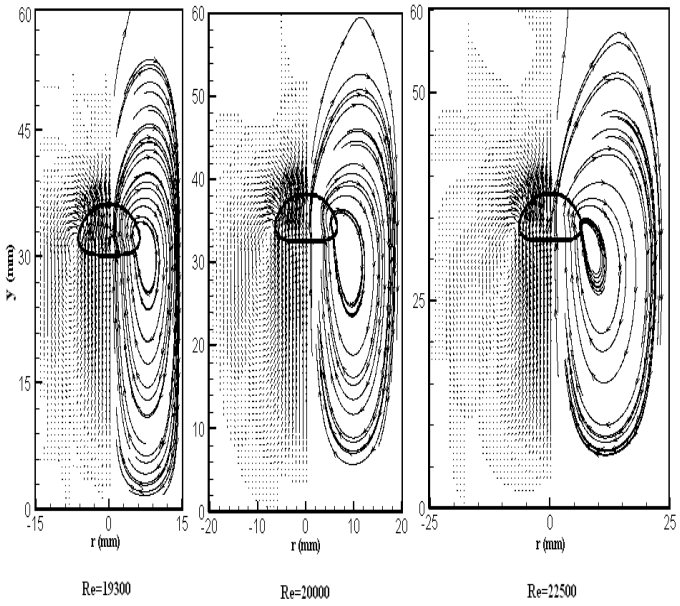

Fig. 3: The effect of tube diameter on the bubble shape and rise velocity

parameters	liquid	gas
density	ρ_l =1000 kg/m^3	ρ_g =10 kg/m^3
viscosity	μ_l=0.1 kg/(m.s)	μ_a=0.001 kg/(m.s)
surface tension	γ =0.0673 N/m,	-
bubble diameter	-	0.01 m

Tab. 3: Data used for the simulation to study the effect of tube diameter.

The effect of the bubble size on terminal velocity is shown in Fig. 4. The rise velocity is made dimensionless using $\Delta\rho g {R_t}^2 / \mu_l$, where R_t is the tube radius; the bubble radius is also made dimensionless using the tube radius as R_b/R_t. This figure shows the comparison between numerical results and measurements [25]. The experiments were performed for systems with small values of *Ca/Bo*, where *Ca* and *Bo* are Capillary number ($Ca = \frac{\mu \vec{V}}{\gamma}$) and Bond number ($Bo = \frac{\Delta\rho g R_t^{\,2}}{\gamma}$), respectively. As seen from the figure, the terminal velocity increases with bubble radius upto a maximum at an intermediate bubble radius of R_b/R_t=0.5. After this point, the terminal velocity decreases with further increase of the bubble radius. This is because the larger retarding effect of the capillary wall begins to overcome the increase in the buoyancy force with increasing the bubble size.

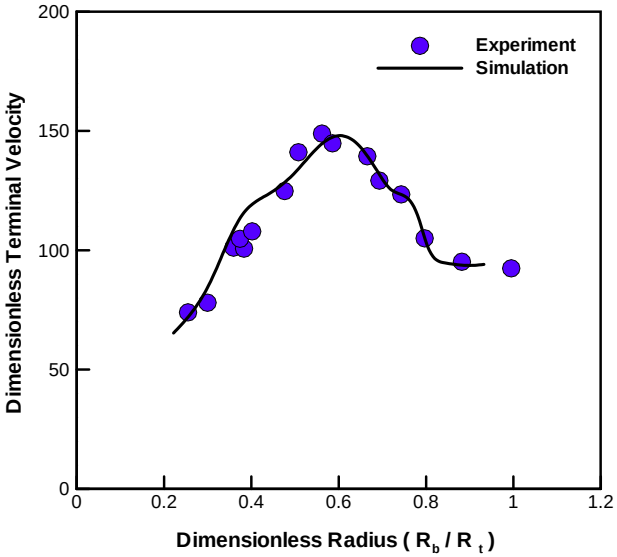

Fig. 4: Dimensionless rise velocity against dimensionless bubble radius.

It is well known that surface tension causes an excess pressure inside a bubble given by the Laplace equation as $\Delta p = 2\gamma / R_b$ for a spherical shape, where γ is the surface tension coefficient and R_b the bubble radius. Figure 5 shows the effect of surface tension on bubble rise velocity. The data used in this simulation are those given in Table 3 except for surface tension which varied from 0.03 N/m to 0.15 N/m. From the figure, it can be clearly seen that the bubble rise velocity increases with liquid surface tension.

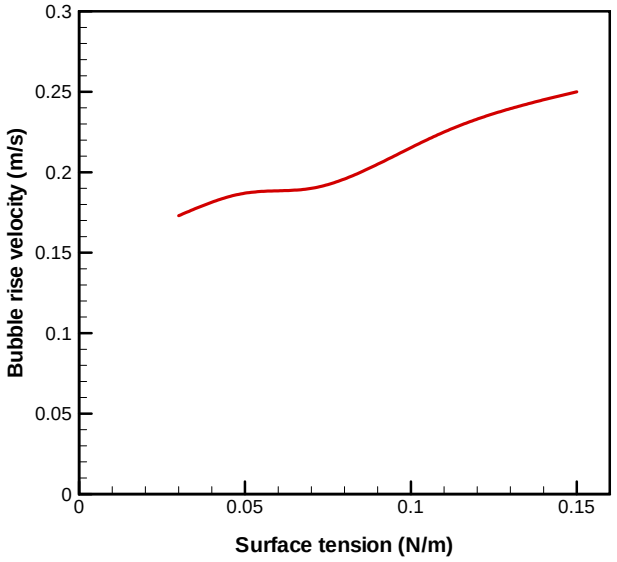

Fig. 5: The variation of bubble rise velocity versus surface tension for a bubble of 0.01 m in diameter.

Figure 6 displays the effect of viscosity on terminal rise velocity for a bubble with an initial diameter of 0.01 m. For a given bubble size, the bubble rise velocity is reduced as viscosity ratio is increased. This result was expected because increasing the viscosity ratio decreases the interfacial motion due to viscous forces. The relative reduction in terminal rise velocity from the maximum to the minimum value also becomes less pronounced as the viscosity ratio increases.

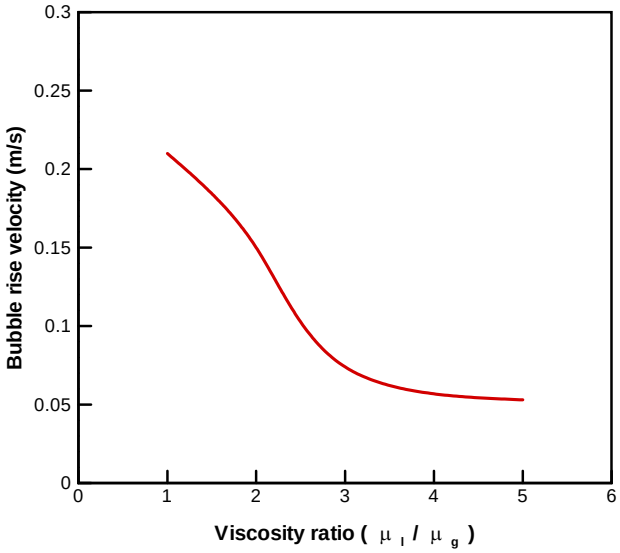

Fig. 6: The variation of bubble rise velocity versus viscosity ratio for a bubble of 0.01 m in diameter.

Bubble Departure from the Free-Surface

In this section, the effect of the bubble departure from the free surface is investigated. When gas bubbles rise through a pool of liquid and approach the free surface, the various violent motions associated with the free-surface breakup generate droplets that may persist in the surrounding gas to constitute a spray. The spray formation by this phenomenon (bubbling at the free surface) is shown in Fig. 7 where the free-surface dynamic behavior after a single bubble departure from the liquid is shown using both numerical model and experiments [26]. A schematic of the important processes during this phenomenon is shown in Fig. 8. A thin film of liquid is formed on top of the bubble before it leaves the free surface. The breakup and disintegration of this film create a spray of droplets with sizes in the order of one tenth of the bubble diameter. The surface waves formed during the free-surface rise propagate inward (toward the center) and outward away from the bubble. An upward jet is formed at the center of the disruption; the disintegration of this jet also creates small droplets. In general, the droplets formed from the disintegration of this jet are bigger in size than those formed from the breakup of the thin film. The material parameters used for the simulations in this section are given in Table 1.

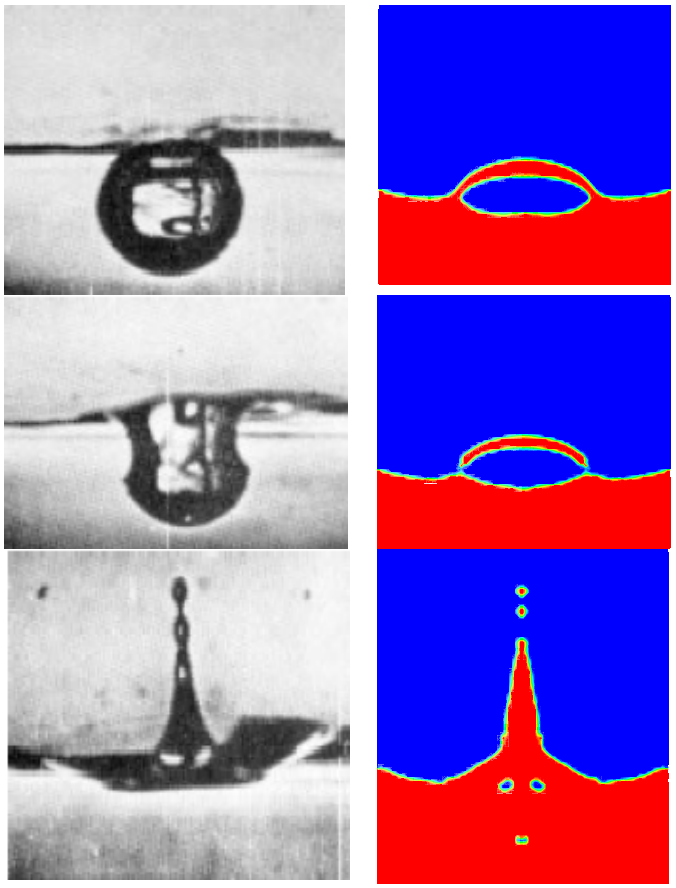

Fig. 7: Qualitative comparison between calculated images and experimental photographs [26] for the deformation of the free surface and formation of a spray during a single bubble departure.

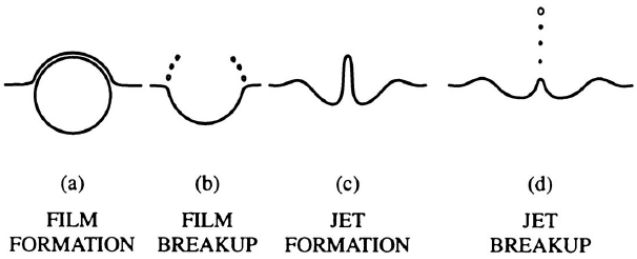

Fig. 8: Stages of a bubble breaking through a free surface

The important effects of the bubble departure on the free surface deformation appear after the bubble left the liquid. As seen from Fig. 7, the liquid rises at the departure point; this phenomenon causes a low speed liquid spray rising from the free surface. The height of the spray is affected by different parameters namely the tube diameter, the initial bubble radius and the distance between the initial bubble location and the free-surface level. Figure 9 shows the effect of the tube diameter (made dimensionless by the bubble diameter *D*) on the height of the free surface spray. As seen from the figure, increasing the tube diameter increases the height of the liquid

rising above the free surface. This result was expected because increasing the tube diameter increases the bubble rise velocity which in turn causes a higher spike.

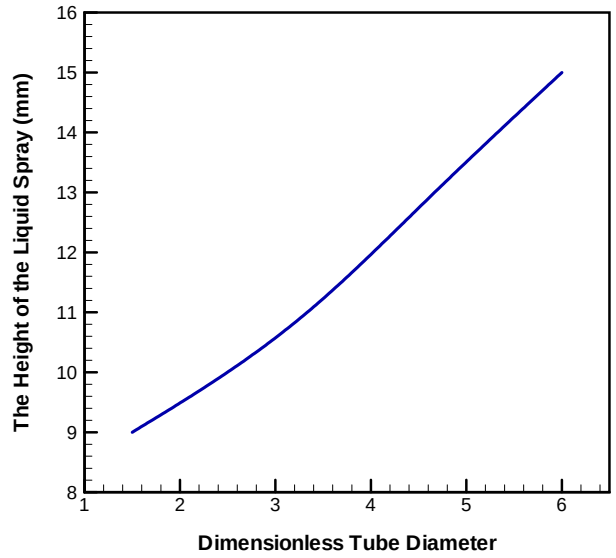

Fig. 9: The variation of the height of the liquid spike versus dimensionless tube diameter.

Figure 10 shows the effect of bubble radius on the height of the spray. From this figure, it can be seen that the height is a linearly increasing function of the bubble radius. The initial bubble center for the simulations shown in this figure was located at a distance beneath the free surface equal to four times as much as the bubble radius.

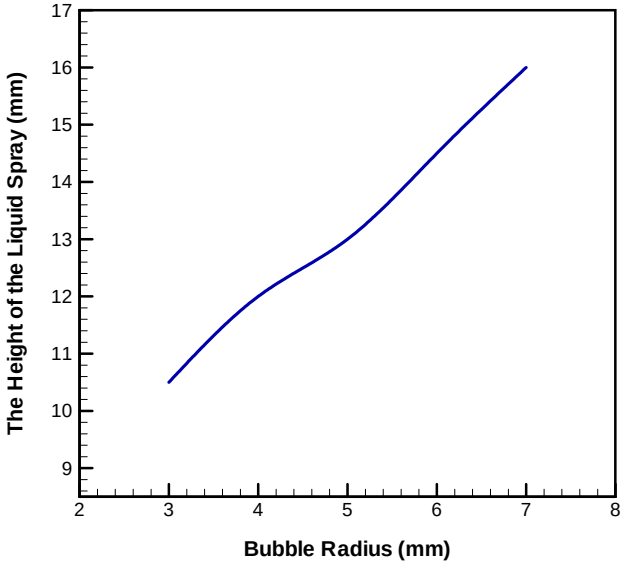

Fig. 10: The variation of the height of the liquid spike versus bubble radius.

CONCLUSION

In this paper, an axisymmetric VOF method was used to simulate the rise and interaction of gas bubbles in a viscous liquid. The model was validated by a comparison between numerical results with available measurements for the bubble deformation and velocity during its rise in a liquid. The effect of increasing diameter on bubble rise velocity was also investigated and compared well with that of the experiment. Next, we investigated the effect of important parameters on the bubble rise velocity. A bubble moving in a narrower tube (smaller diameter) was found to reach a smaller rise velocity. Surface tension and viscosity had adverse effects on the bubble movement. While increasing surface tension raised the bubble rise velocity, increasing liquid viscosity had an opposite effect. Finally, the effect of the bubble departure on the liquid free surface was investigated. The three parameters controlling the height of the liquid above the free surface (spray formation) were found to be the tube diameter; the bubble radius; and the distance between the initial bubble center and the free-surface level. Increasing the tube diameter and the bubble radius increased the height of the spray.

REFERENCES

[1] Sussman, M. Smereka, P. and Osher, S., "A level set approach for computing solutions to incompressible two-phase flow," *J. Comput. Phys*, Vol. 114, pp. 146-159, 1994.

[2] Sethian, J.A., "Level Set Methods," *Cambridge University Press, Cambridge*, UK, 1996.

[3] Sussman, M., and Smereka, P., "Axisymmetric free boundary problems," *J. Fluid Mech.*, Vol. 341, pp. 269–294, 1997.

[4] Sussman, M, and Fatemi, E., "An efficient interface-preserving level set redistancing algorithm and its application to interfacial incompressible fluid flow," *SIAM J. Sci. Comput.*, Vol.20, pp.1165-1191, 1999.

[5] Fedkiw, R., and Osher, S., "Level-set methods: an overview and some recent results," *J. Comput. Phys*, Vol. 169, p. 463, 2001.

[6] Pasandideh-Fard, M. and Roohi, E. "A Computational Model for Cavitation Using Volume-of-Fluid Method," *14th Annual Conf. of CFD Canada, Kingston*, 2006.

[7] Noh, WF, and Woodward, PR., "SLIC (Simple Line Interface Calculation) method," In: Van Vooren AI, Zandbergen PJ, eds. Lecture Notes inPhysics. Vol. 59. *Berlin: Springer-Verlag*; 330, 1976.

[8] Hirt, C.W., and Nichols, B.D., "Volume of fluid (VOF) method for the dynamics of free boundaries," *J. Comput. Phys*, Vol. 39, p. 201, 1981.

[9] Youngs, DL., “Time-dependent multi-material flow with large fluid distortion,” In: Morton KW, Bianes MJ, eds. *Numerical methods for fluid dynamics.* New York, NY: *Academic Press*, pp. 273-285, 1982.

[10] Rudman, M., “Volume-tracking methods for interfacial flow calculations,” *International journal of numerical methods in fluids*, Vol. 24, pp. 671–691, 1997.

[11] Unverdi, SO, and Tryggvason G. “A front-tracking method for viscous, incompressible multi-fluid flows,” *J. Comput. Phys*, Vol. 100, pp. 25-37, 1992.

[12] Esmaeeli, A., and Tryggvason, G., “Direct numerical simulation of bubble flows,” Part I. Low Reynolds number arrays. *J. Fluid Mech.*, Vol. 377, pp. 313–345, 1998.

[13] Esmaeeli, A., and Tryggvason, G., “Direct numerical simulation of bubble flows,” Part II. Moderate Reynolds number arrays. *J. Fluid Mech.*, Vol. 385, pp. 325–358, 1998b.

[14] Van Sint Annaland, M., Dijkhuizen, W., Deen, N. G., and Kuipers, J. A. M., “Numerical simulation of behavior of gas bubbles using a 3-D front-tracking method, ” *AIChE J*, Vol. 52, pp. 99–110, 2006.

[15] Herring, C. “Theory of the pulsations of the gas bubble produced by an underwater explosion,” In: Hartmann GK, Hill EG, editors. Underwater explosion research, vol. II. Washington, DC: Office of Naval Research; 1949.

[16] Taylor, GI. “Vertical motion of a spherical bubble and the pressure surrounding it,” In: Hartmann GK, Hill EG, editors. Underwater explosion research, vol. II. Washington, DC: Office of Naval Research; 1942.

[17] Lenoir, M. Calcul nume´rique de l’implosion d’une bulle de cavitation au voisinage d’une paroi ou d’une surface libre. J Me´c; 15(5):725–51, 1976.

[18] Blake, JR, and Gibson DC. “Growth and collapse of a vapour cavity near a free surface,” *J. Fluid Mech.*, Vol. 111, pp. 123–40, 1981.

[19] Kucera, A. and Blake, JR. “Approximate methods for modeling cavitation bubbles near boundaries,” Bull Aust Math Soc, Vol.41, pp.1–44, 1990.

[20] Cox, E. “The source signature due to the close interaction of marine seismic airguns,” PhD Thesis, The University of Birmingham, 2003.

[21] Bussmann M., Mosthghimi J., and Chandra S., "On a Three-Dimensional Volume Tracking Model of Droplet Impact", Phys. Fluid, Vol. 11, p. 1406, 1999.

[22] Clift, R, and Grace, J.R., and Weber, M., 1978, Bubbles, drops and particles, Academic Press, New York.

[23]Grace, JR., “Shapes and velocities of bubbles rising in infinite liquids,” *Trans ICHemE.*:51:116-120, 1973.

[24] Sabisch, W., Worner, M., Grotzbach, G., Cacuci, D.G. Driedimensionale numerische Simulation von aufsteigenden Einzelblasen und Blasenschwarmen mit einer Volume-of Fluid-Methode. Chemie Ingenieur Technik 73, 368–373, 2001.

[25] Matroushi, Eisa A., Ineteraction and coalescence of bubbles and drops moving through a tube, Ph.D. Pennsylvania State University, 2000.

[26] Blanchard, D.C., “The electrification of the atmosphere by particles from bubbles in the sea,” *Progr. in Oceanography*, Vol. 1, p. 72, 1963.